Biochemistry

pubs.acs.org/biochemistry Communication

Computational Evolution of Anti-PD-1 Antibodies Induces Structural Refolding for High-Affinity Interactions

Yuanjun Shi, Yeil Kim, Pulan Liu, Jimin Wang,* Shaogeng Tang,* and Victor S. Batista*

Cite This: https://doi.org/10.1021/acs.biochem.5c00574 Read Online

ACCESS | Metrics & More | Article Recommendations | Supporting Information

ABSTRACT: Checkpoint inhibitors targeting the PD-1/PD-L1 axis are key immunotherapies, but the dynamic and flexible nature of PD-1 complicates rational antibody engineering. Here, we use computational saturation mutagenesis, AlphaFold prediction, and molecular dynamics (MD) simulations to evolve pembrolizumab variants with suitable binding. Seven engineered antibodies form additional salt bridges and hydrophobic contacts via refolding of both the antibody and the PD-1 interface. One variant, m7p.5, displays improved biphasic kinetics and high-affinity binding ($K_{D,apparent}$ = 62 pM). Structural changes include an α-helix to loop transition in the antibody heavy chain and a 4.6-Å Cα shift of a PD-1 loop. These results show that computational evolution can access binding modes inaccessible to traditional rigid structural design, enabling high-affinity antibodies for flexible targets. It is demonstrated that our integrated computational approaches including MD simulations can generate new picomolar high-affinity antibodies targeting specific epitopes of proteins that may be intrinsically flexible and are difficult to target with reasonable computational cost, which would be far less than an experimental cost for finding new antibodies with equivalent binding affinities. This study provides a new tool that can be combined with other artificial-intelligence-based antibody generation against PD-1 from the existing anti-PD-1 antibody library with broad applications in protein−protein interactions.

Programmed death ligand-1 (PD-L1) is a type I transmembrane protein and a key immune checkpoint ligand involved in tumor immune evasion.[1,2] Immunotherapies targeting the PD-1/PD-L1 axis—particularly monoclonal antibodies—have revolutionized cancer treatment, with static structural insights from X-ray crystallography playing a central role in their development.[3−5] Despite the success of therapeutics such as pembrolizumab, which exhibits picomolar binding affinity (K_D),[6] further affinity enhancement remains difficult. This is largely due to the conformational plasticity of the PD-1 epitope, especially its FG loop, which poses a significant barrier to traditional structure-based antibody optimization.

Here, we present a computational evolution pipeline designed to overcome the conformational plasticity limitation. The approach employs saturation mutagenesis at pembrolizumab interface residues, guided by AlphaFold2 structural predictions and refined via molecular dynamics (MD) simulations.[7] This strategy yielded seven high-affinity antibody variants featuring new interprotein salt bridges and hydrophobic interactions, arising from coordinated structural rearrangements in both PD-1 and the antibody. Notably, variant m7p.5 exhibited biphasic binding kinetics and enhanced affinity ($K_{D,apparent}$ = 62 pM) likely driven by an α-helix to loop transition in the antibody heavy chain. These findings demonstrate that computational evolution can access alternative binding modes beyond the reach of traditional rigid design approaches, enabling the development of high-affinity antibodies against conformationally dynamic targets.

Equilibrated pembrolizumab/PD-1 complex structures were derived from MD-simulated ED maps. Starting from the published crystal structure of the binary complex of pembrolizumab with PD-1 (PDB code 5GGS at 2 Å resolution),[8] random saturation mutations were introduced using PyMol.[9] Structures were filtered via AlphaFold2[7] and then simulated in explicit solvent using the OPLS force field as implemented in Maestro with periodic boundary conditions;[10] 400 ns production runs were analyzed for hydrogen bonding, hydrophobic contacts, and root-mean-square deviation (RMSD).[11−14] An extended description of materials and methods can be found in the Supporting Information (SI).

IgG variants were expressed in Expi293F cells and purified using Protein A columns (see Table S6 for cloning and expression sequences). Binding to biotinylated PD-1-Fc was measured with an Octet R8 instrument (Sartorius). Association/dissociation were analyzed using two-phase exponential fitting (SI).

Biotinylated PD-1-Fc was immobilized and exposed to antibodies followed by PD-L1. No additional signal indicated competitive inhibition. Interpretation of kinetic parameters for pseudo-fast-order reaction follows earlier work.[15,16] Briefly, the association rate in each phase is described by $k = k_{on}[Ab]_0 - k_{off}$, where [Ab] is the concentration of antibodies used for the assay. In dissociation reactions, the dissociation rate is the same as the off rate constant k_{off} and independent of the antibody concentration $[Ab]_0$, where k_{on} and k_{off} are rate

Received: September 16, 2025
Revised: January 22, 2026
Accepted: January 26, 2026

constants. Once the antibody concentration is known, it is $k_{on} = [k + k_{off}]/[Ab]_0$. The binding affinity $K_D = k_{off}/k_{on} = [k_{off}/(k + k_{off})]$ $[Antibody]_0$ is determined using the fitted parameters in the fast association phase and the slow dissociation phase.

We selected 7 interface residues of pembrolizumab—T31, S32, L50, R96 in the light chain and T28, T30, S54 in the heavy chain—for computational saturation mutagenesis (Figure 1, Figure S1–S5, Table S1). All mutated complexes

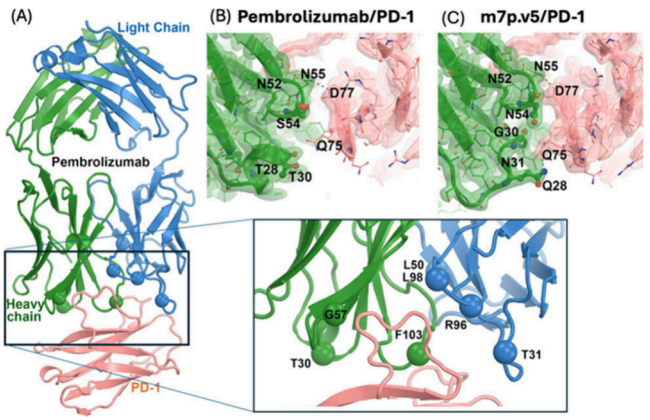

Figure 1. (A) MD-derived equilibrium complex of pembrolizumab with PD-1 and selection of seven interface targets of pembrolizumab for saturation random mutagenesis marked by large spheres. (B,C) Comparison of epitope contacts in the pembrolizumab/PD-1 complex structure and the m7p.v5/PD-1 complex structure, shown as MD-derived electron density (ED) maps contoured at 4σ. See Figure S1 for close-up view MD-derived ED maps for the parental pembrolizumab-PD-1 complex and detailed interactions at the interface, and Figure S2–S5 for other interactions with designed antibodies.

were assessed using AlphaFold2 for structural plausibility, and the top 10 variants (m7p.0–m7p.9) were evaluated with 400 ns explicit-solvent MD simulations (Table S1, Figure S6).[7]

The simulations revealed that variants m7p.3–m7p.7 and m7p.9 retained interface complementarity and were very stable across MD trajectories (Figure 1, S2–S5). As detailed in Figure 1 and supported by the well-defined MD-derived electron density (ED) maps, these variants formed some new persistent interactions that are not present in the parental pembrolizumab complex.

MD analysis revealed that all engineered variants introduced new interprotein salt bridges that are not present in the parental complex. In particular, T31D and R96D formed multiple H-bonds with PD-1 R86, which are not present in the parental pembrolizumab complex (Table S2-S5), stabilizing its FG loop (residues 85–90) into a new defined rotamer. These interactions were correlated with higher binding stability, as confirmed by cumulative hydrogen bond occupancies over simulation time (Figure S6, Tables S2–S5). These conformations include a weak paired arginine–arginine interaction, which is a well-documented type of interaction known as a magic arginine–arginine pair.[17,18] It is noted that the charge reversion mutation such as R96D would not typically be considered a viable choice in the traditional approach of affinity maturation or rigid structure-based protein design.

Another key structural change was observed in the G26–T30 region of the heavy chain CDR1. In pembrolizumab, this region adopts an α-helical turn with minimal PD-1 contact, not making significant interactions with PD-1. In contrast, variants with T28Q and T30G (e.g., m7p.5) adopted a compact loop, forming hydrogen bonds with PD-1 Q75 and D77 (Figure 1). This induced a conformational shift in PD-1's FG loop near S73 by approximately 4.6 Å, enabling new hydrophobic contacts—particularly in variants carrying S32F/Y/H substitutions (Table S5).

Biolayer interferometry (BLI) was used to determine the binding properties of the engineered antibodies. Variants m7p.3–m7p.7 and m7p.9 exhibited strong association responses and formed stable complex formation with PD-1 (Figure 2, Figure S7, S8). Association curves followed a

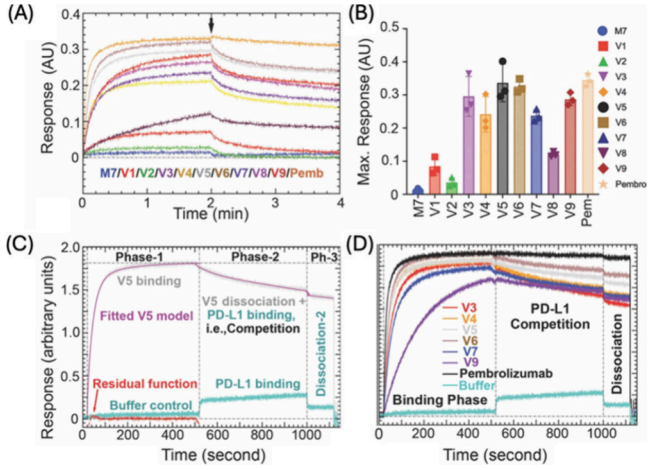

Figure 2. Binding assay of designed anti-PD-1 antibodies using biolayer interferometry (BLI) methods. (A) The sensor graphs for association of the m7p.0, m7p.1 (V1) to m7p.9 (V9) and pembrolizumab to immobilized PD-1 for 2 min followed by dissociation for other 2 min. (B) Maximal response units from three independent measurements. (C,D) Typical competition assay in three phases. Phase-1 is for the binding of V5 or buffer control (panel C) or other designed anti-PD-1 antibodies plus pembrolizumab control (panel D). Phase-2 is for dissociation of antibodies and binding of PD-L1. Phase-3 is for dissociation in buffer. Fitted models for V5 and residual function are also shown (panel C). See Figure S7 and S8 for detailed fitting of biphasic kinetic parameters.

biphasic kinetic profile, best fit by two exponential components—fast and slow binding phases (Figure 2, Figure S7, S8). For example, m7p.5 had a fast association rate of 14.4 min^{-1}, a slower phase of 2.7 min^{-1}, and $K_{D,apparent}$ = 62 pM—comparable to pembrolizumab (42 pM, see Table 1).

Dissociation phases also followed biphasic behavior (Figure S8B), where slow off-rates dominated. For m7p.5, 88% of the complex dissociated via a slow phase, suggesting enhanced kinetic trapping via the engineered interfacial network. This

Table 1. Binding Kinetics of Selected Variants vs Pembrolizumab

Antibody	k_1 (m^{-1})	k_2 (m^{-1})	$K_{D,app.}$ (pM)
Pembrolizumab	15.8	2.5	42
m7p.5	14.4	2.7	62
m7p.4	16.0	2.9	56
m7p.3	13.3	2.1	68
m7p.6	13.2	2.3	68
m7p.7	12.2	2.2	74
m7p.9	10.5	2.0	85

https://doi.org/10.1021/acs.biochem.5c00574
Biochemistry XXXX, XXX, XXX–XXX

kinetic profile may reflect the multistep structural docking observed in MD.

Three-phase binding competition assays showed that all high-affinity variants block binding of PD-L1 to PD-1. In Phase 1, association with designed antibodies occurs. In Phase 2, no additional signal was observed upon PD-L1 introduction, indicating that association with PD-1 occurs only with the uncomplexed fraction of PD-1, which is either the uncomplexed PD-1 from Phase 1 to start with or after dissociation of bound antibody variants in Phase 1, i.e., PD-L1 shares the same or overlapping binding sites of designed antibodies. Phase 3 dissociation phases were for both PD-L1 and designed antibodies (in Phase 2), further validating their direct competition. These results confirm that, despite sequence and structural divergence from the parental antibody, the engineered variants retain the desired therapeutic mechanism of action.

This study shows that our computational evolution—combining saturation mutagenesis, structural prediction, and MD simulations—can produce antibody variants with new structural and kinetic properties. Importantly, the variants refold themselves and their antigen targets to establish new interactions that would be invisible to traditional design. This method offers a generalizable framework for engineering antibodies against flexible or poorly structured epitopes.

In conclusion, it has been demonstrated that a combination of computational saturation mutations, AlphaFold complex predictions, and molecular dynamics simulations can solve antibody affinity maturation problems. Although this is a proof-of-principle study, beginning with a high affinity antibody pembrolizumab, it could work better with low-affinity antibodies, which should have much larger room for affinity improvement. It might be relatively straightforward and inexpensive both experimentally and computationally to generate many low-affinity antibodies against a given specific antigen; this study could pave a new path toward affinity maturation of these antibodies to generate high-affinity antibodies.

■ ASSOCIATED CONTENT

Supporting Information

The Supporting Information is available free of charge at https://pubs.acs.org/doi/10.1021/acs.biochem.5c00574.

Extended Method Descriptions, Supporting Figures S1−S8, Supporting Tables S1−S6, and Supporting References (1−13) (PDF)

Computer folder archive containing the equilibrium atomic coordinates of 8 PD-1 complexes with each of seven designed mutants and the parental pembrolizumab derived from the MD simulation, two selected MD-ED maps for the complexes with variant m7p.5 or pembrolizumab, and other useful setup scripts (ZIP)

■ AUTHOR INFORMATION

Corresponding Authors

Jimin Wang − *Department of Molecular Biophysics and Biochemistry, Yale University, New Haven, Connecticut 06520, United States;* orcid.org/0000-0002-4504-8038; Email: jimin.wang@yale.edu

Shaogeng Tang − *Department of Molecular Biophysics and Biochemistry and Wu Tsai Institute, Yale University, New Haven, Connecticut 06520, United States;* Email: shaogeng.tang@yale.edu

Victor S. Batista − *Department of Chemistry, Yale University, New Haven, Connecticut 06511, United States;* orcid.org/0000-0002-3262-1237; Email: victor.batista@yale.edu

Authors

Yuanjun Shi − *Department of Chemistry, Yale University, New Haven, Connecticut 06511, United States;* orcid.org/0000-0002-9240-6950

Yeil Kim − *Department of Pharmacology, Yale University, New Haven, Connecticut 06520, United States;* orcid.org/0009-0005-8816-9883

Pulan Liu − *Department of Molecular Biophysics and Biochemistry, Yale University, New Haven, Connecticut 06520, United States*

Complete contact information is available at: https://pubs.acs.org/10.1021/acs.biochem.5c00574

Author Contributions

V.S.B., S.T., and J.W. conceived the idea, Y.S., Y.K., and P.L. carried out studies, Y.S. and J.W. carried out analysis and wrote the draft manuscript with input from all authors.

Notes

The authors declare no competing financial interest.

■ ACKNOWLEDGMENTS

This study was partially funded by the National Institutes of Health under Grants No. R01 GM136815 (V.S.B.) and R00HD104924 (S.T.). Computation time was also provided by the National Energy Research Scientific Computing Center (NERSC) under Grant No. M3807.

■ ABBREVIATIONS

PD-1; programmed death protein-1; PD-L1; programmed death ligand protein 1

■ REFERENCES

(1) Lin, X.; Kang, K.; Chen, P.; Zeng, Z.; Li, G.; Xiong, W.; Yi, M.; Xiang, B. Regulatory mechanisms of PD-1/PD-L1 in cancers. *Mol. Cancer* **2024**, *23* (1), 108. From NLM Medline.

(2) Wang, Q.; Wu, X. Primary and acquired resistance to PD-1/PD-L1 blockade in cancer treatment. *Int. Immunopharmacol* **2017**, *46*, 210−219. From NLM Medline.

(3) Jiang, M.; Liu, M.; Liu, G.; Ma, J.; Zhang, L.; Wang, S. Advances in the structural characterization of complexes of therapeutic antibodies with PD-1 or PD-L1. *MAbs* **2023**, *15* (1), 2236740. From NLM Medline.

(4) Jiang, Y.; Chen, M.; Nie, H.; Yuan, Y. PD-1 and PD-L1 in cancer immunotherapy: clinical implications and future considerations. *Hum Vaccin Immunother* **2019**, *15* (5), 1111−1122. From NLM Medline.

(5) Zak, K. M.; Grudnik, P.; Magiera, K.; Domling, A.; Dubin, G.; Holak, T. A. Structural Biology of the Immune Checkpoint Receptor PD-1 and Its Ligands PD-L1/PD-L2. *Structure* **2017**, *25* (8), 1163−1174.

(6) Na, Z.; Yeo, S. P.; Bharath, S. R.; Bowler, M. W.; Balikci, E.; Wang, C. I.; Song, H. Structural basis for blocking PD-1-mediated immune suppression by therapeutic antibody pembrolizumab. *Cell Res.* **2017**, *27* (1), 147−150.

(7) Yang, Z.; Zeng, X.; Zhao, Y.; Chen, R. AlphaFold2 and its applications in the fields of biology and medicine. *Signal Transduct Target Ther* **2023**, *8* (1), 115. From NLM Medline.

(8) Lee, J. Y.; Lee, H. T.; Shin, W.; Chae, J.; Choi, J.; Kim, S. H.; Lim, H.; Won Heo, T.; Park, K. Y.; Lee, Y. J.; et al. Structural basis of

checkpoint blockade by monoclonal antibodies in cancer immunotherapy. *Nat. Commun.* **2016**, *7*, 13354.
(9) Delano, W. L. *PyMol*. Schrodinger, Inc. http://pymol.org/.
(10) Case, D. A.; Aktulga, H. M.; Belfon, K.; Cerutti, D. S.; Cisneros, G. A.; Cruzeiro, V. W. D.; Forouzesh, N.; Giese, T. J.; Gotz, A. W.; Gohlke, H.; et al. AmberTools. *J. Chem. Inf Model* **2023**, *63* (20), 6183−6191. From NLM PubMed-not-MEDLINE.
(11) Shi, Y.; Wang, J.; Batista, V. S. Translocation pause of remdesivir-containing primer/template RNA duplex within SARS-CoV-2's RNA polymerase complexes. *Front Mol. Biosci* **2022**, *9*, 999291.
(12) Wang, J.; Shi, Y.; Reiss, K.; Maschietto, F.; Lolis, E.; Konigsberg, W. H.; Lisi, G. P.; Batista, V. S. Structural insights into binding of remdesivir triphosphate within the replication-transcription complex of SARS-CoV-2. *Biochemistry* **2022**, *61* (18), 1966−1973.
(13) Wang, J.; Shi, Y.; Reiss, K.; Allen, B.; Maschietto, F.; Lolis, E.; Konigsberg, W. H.; Lisi, G. P.; Batista, V. S. Insights into binding of single-stranded viral RNA template to the replication-transcription complex of SARS-CoV-2 for the priming reaction from molecular dynamics simulations. *Biochemistry* **2022**, *61* (6), 424−432.
(14) Wang, B.; Gallolu Kankanamalage, S.; Dong, J.; Liu, Y. Optimization of therapeutic antibodies. *Antib Ther* **2021**, *4* (1), 45−54. From NLM PubMed-not-MEDLINE.
(15) Du, Y. Binding curve viewer: visualizing the equilibrium and kinetics of protein-ligand binding and competitive binding. *J. Chem. Inf. Model.* **2024**, *64* (10), 4180−4192.
(16) Pollard, T. D. A guide to simple and informative binding assays. *Mol. Biol. Cell* **2010**, *21* (23), 4061−4067. From NLM Medline.
(17) Magalhaes, A.; Maigret, B.; Hoflack, J.; Gomes, J. A. N. F.; Scheraga, H. A. Contribution of Unusual Arginine-Arginine Short-Range Interactions to Stabilization and Recognition in Proteins. *J. Protein Chem.* **1994**, *13* (2), 195−215.
(18) Vazdar, M.; Heyda, J.; Mason, P. E.; Tesei, G.; Allolio, C.; Lund, M.; Jungwirth, P. Arginine "Magic": Guanidinium Like-Charge Ion Pairing from Aqueous Salts to Cell Penetrating Peptides. *Acc. Chem. Res.* **2018**, *51* (6), 1455−1464. From NLM Medline.

https://doi.org/10.1021/acs.biochem.5c00574
Biochemistry XXXX, XXX, XXX−XXX